Synthesis of rGO/TiO$_2$ Nanocomposite for the Efficient Photocatalytic Degradation of RhB Dye

Vikash Kumar, Ajay Bansal and Renu Gupta

Abstract In this work, the successful synthesis of reduced graphene oxide–TiO$_2$ (rGO/T) photocatalysts with various concentrations of GO (5, 10, 15, and 20 wt%) has been reported. The synthesis of rGO/T photocatalysts was done by the photo-assisted reduction of GO to rGO using ultraviolet radiation followed by the hydrothermal deposition of rGO onto the TiO$_2$. The synthesized photocatalysts were characterized by field-emission scanning electron microscopy (FE-SEM), X-ray diffraction (XRD), and energy dispersive X-ray spectroscopy (EDXs) techniques. The photocatalysts were used for the photodegradation of Rhodamine B (RhB) dye. The photocatalytic degradation of RhB dye of 10 ppm was successfully carried out under UV light, as well as solar light irradiation over rGO/T photocatalysts. Here, the influence of GO over the photoactivity of TiO$_2$ was explored. It was found that the synthesized rGO/T photocatalysts exhibit enhanced photocatalytic efficiency as compared to unmodified TiO$_2$. The rate of photodegradation of RhB dye was successfully fitted by Langmuir–Hinshelwood kinetic model.

Keywords TiO$_2$ · Graphene oxide · rGO/T · Photocatalysis · Rhodamine B

V. Kumar · A. Bansal (✉) · R. Gupta
Department of Chemical Engineering, Dr. B. R. Ambedkar National Institute of Technology, Jalandhar 144011, India
e-mail: bansala@nitj.ac.in

V. Kumar
e-mail: vikash.jaiswal15@gmail.com

R. Gupta
e-mail: bansalr@nitj.ac.in

1 Introduction

The discharge of a huge quantity of colored dyes from various industries such as textile, plastic, paper, printing, pharmaceutical, and food industry into water bodies are the life-threatening health hazard to aquatic as well as human life. These dyes being toxic in nature are imposing a serious threat to the environment (Chang et al. 2009). Rhodamine B (RhB) is one of the very common water-soluble organic dyes and is extensively used as a colorant in the textile and food industries, as well as a biological stain in biomedical laboratories. RhB has been banished to use in the food industry for many years due to its suspected carcinogenic nature. However, with the development of industry and the illegal discharge, RhB still has the chances to enter the aliment chain to hazard human health. It is therefore essential to remove these dyes from dye effluents prior to their discharge into the receiving water bodies (Rani et al. 2016; Shen and Gondal 2017; Yu et al. 2004; Li et al. 2014a, b; Carneiro et al. 2016). To date, several treatment methods such as chemical oxidation, coagulation, biological treatment, ozonolysis, and adsorption have been extensively explored for the removal of organic pollutants from industrial effluents, but all such methods suffer from a number of drawbacks such as very low removal efficiency, generation of secondary pollutant, high chemical consumption, and high cost of treatment (Carneiro et al. 2016; Oseghe et al. 2014). Photocatalysis using semiconductor nanocomposites is involved in a group of waste treatment methods called advanced oxidation processes (AOPs) (Carneiro et al. 2016). AOPs are recommended when wastewater components have a high chemical stability and/or low biodegradability. A chemical wastewater treatment using AOPs can produce the complete mineralization of pollutants to CO_2, water, and inorganic compounds (Thiruvenkatachari et al. 2008).

Titanium dioxide (TiO_2) has gained intensive attention due to their strong oxidizing power, physicochemical stability, non-toxicity, low-cost production and eco-friendly nature (Friedmann et al. 2010) (Krejčíková et al. 2012; Nakata and Fujishima 2012; Gnanasekaran et al. 2015). However, the photocatalytic activity of TiO_2 is strongly influenced by its structural properties such as morphology, crystalline phase, particle size, surface hydrophilicity, and oxygen vacancy concentration (Shao et al. 2013). The efficiency of the photocatalytic reaction of TiO_2 gets significantly reduced owing to its wide band gap energy of 3.2 eV and high electron-hole recombination rate. Thus, restricting the electron-hole pair recombination and extending the light absorption to the longer wavelength are the key factors to improve the photocatalytic activity of TiO_2 (Chen and Mao 2007; Abdel-Messih et al. 2013; Yadav et al. 2017). Consequently, several attempts have been made to improve the performance of TiO_2 such as modifying it with carbonaceous materials like CNTs, Fullerene, graphene, or graphene oxide. Doping or immobilization of TiO_2 over the surface of carbon extends the absorption range of TiO_2 to the visible region. In addition, the nonpolar, nonreactive, and nontoxic natures of carbon materials play a significant role in the treatment of wastewater containing complex toxic organic compounds (Fang et al. 2017).

Graphene oxide (GO), a two-dimensional sp^2 hybridized carbonaceous material, which has been extensively investigated because of its unique structure, large surface area (2630 m^2/gm), high mechanical strength, and good physicochemical stability. Benefiting from the large surface area, superior electronic, thermal, and optoelectronic properties, GO has gained great attention in various fields such as catalysts, sensors, supercapacitors, and energy devices (Dubey et al. 2014; Lin et al. 2015; Lorestani et al. 2015; Li et al. 2014a, b; Štengl et al. 2013). The synthesis of GO-TiO$_2$ composite is regarded as a significantly important approach for improving the performance of photocatalysts. The hybridization of GO-TiO$_2$ can reduce the recombination of photogenerated electron-hole pairs, extend the light absorption to the visible light region, and accelerate the transfer rate of charge carriers (Lv et al. 2012; Kumar et al. 2015; Hamandi et al. 2017).

To explore the influence of GO over photocatalytic activity of TiO$_2$, the studies have been made on the degradation of RhB dye using GO-supported TiO$_2$ nanocomposites. The effects of various parameters such as light source, catalyst dosage, and type of catalysts have also been investigated.

2 Methodology

2.1 Preparation of Graphene Oxide

GO was prepared by the oxidation of natural graphite powder according to modified Hummer's method. Typically, 2 gm of graphite powder and 1 gm of sodium nitrate were added to 80 ml of concentrated H$_2$SO$_4$ in a 2000 mL beaker maintained at 0 °C under continuous agitation. After 10 min, 12 gm of KMnO$_4$ was added slowly to the above reaction mixture by keeping the reaction temperature below 20 °C. Successively, the reaction system was transferred to a 40 ± 3 °C water bath and vigorously stirred for about 2 h. At the end of 2 h, 40 ml of deionized water (dH$_2$O) was added slowly to the reaction mixture causing violent effervescence and an increase in temperature. The solution is maintained for 15 min at 90 ± 3 °C under agitation. The excess KMnO$_4$ was removed by the addition of 6 ml of 30% H$_2$O$_2$. The yellow bright solution was filtered and washed three–four times with 1400 ml of dH$_2$O followed by 1:10 HCl aqueous solution. The resulting solid was dried in vacuum at 100 °C.

2.2 Preparation of TiO$_2$

In a typical synthesis, 5 ml of titanium (IV) isopropoxide (TTIP) was mixed dropwise in a vigorously stirred 6 ml isopropanol. The resulting mixture was stirred for 15 min and followed by the dropwise addition of 75 ml of dH$_2$O. The addition of dH$_2$O to the above solution resulted in a solution containing a white precipitate. Then, the

temperature knob was adjusted so that the temperature of the solution becomes 80 °C. After stirring at 80 °C for 1 h 2.5 ml of acetic acid was added and continued to stir for 5 h. Then, 1 ml of nitric acid was added for peptidization and the resulting solution was further stirred for 2 h and cooled naturally to room temperature. The as-formed solution was oven dried at 60 °C. The dried powder was crushed in the mortar to make it fine powder, and then this powder was finally annealed at 500 °C for 3 h.

2.3 Synthesis of rGO-TiO$_2$ Photocatalyst

In a typical synthesis process, 500 mg of TiO$_2$ np powder was dispersed in absolute ethanol solution by vigorous stirring for 1 h exposed under UV radiation to store the electrons inside the TiO$_2$ np. Then, GO with different mass ratios (5, 10, 15, and 20 wt%, respectively) was added to the TiO$_2$ np solution. The GO-TiO$_2$ suspension was stirred under UV exposure for another 2 h in order to reduce GO to rGO. The resulting dispersions were subjected to hydrothermal treatment in an autoclave for 2 h. During the hydrothermal process, the partial reduction of GO to reduced graphene oxide (rGO) and the deposition of rGO onto the TiO$_2$ were simultaneously achieved. Finally, the resulted nanocomposites were recovered by centrifugation, followed by washing and drying in oven 100 °C to get the 5-rGO/T, 10-rGO/T, 15-rGO/T, and 20-rGO/T nanocomposites.

2.4 Photocatalyst Characterization

X-Ray Powder Diffraction analysis was performed at room temperature with X'Pert Pro Diffractometer equipped with X'Celerator solid-state detector using Cu-K α radiation ($\lambda = 1.54060$ Å) to observe the crystalline structure and phase composition of the photocatalysts synthesized. The surface morphology and size of the samples were investigated by Field-Emission Scanning Electron Microscope (Carl Zeiss Ultra Plus) coupled with Energy dispersive X-ray spectroscopy (EDXs).

2.5 Photocatalytic Activity Test

The photocatalytic activities of synthesized photocatalysts were evaluated by photodegradation of RhB. The reaction was carried out in batch mode at the initial RhB concentration of 10 ppm under UV and solar light, irrespective of pH of the dye solution. In all the experiments, the volume of dye solution used was 100 ml. Before the irradiation, the suspensions were magnetically stirred in dark for 30 min to reach the

adsorption–desorption equilibrium of RhB dye. The RhB concentration after various time intervals were estimated using the following equation:

$$\% \text{ RhB Degradation } = \frac{C_o - C_t}{C_o} \times 100\%$$

where C_o is the initial RhB concentration and C_t is the concentration after various time intervals (t).

3   Results and Discussion

3.1   FE-SEM

The field-emission scanning electron micrographs of the samples synthesized are depicted in Fig. 1. FE-SEM was done to inspect the topography of the samples synthesized. It is observed from Fig. 1a that GO has a layered structure with cascades of folds, which is due to the introduction of oxidizing functional groups between interlamination of graphite. The different degrees of wrinkles are also observed over the sheets of graphene oxide due to the absence of functional groups. Figure 1b shows agglomerated particles of TiO$_2$ having spherical morphology and rough surfaces. Figure 1c–f shows the micrographs of 5-rGO/T, 10-rGO/T, 15-rGO/T, and 20-rGO/T, respectively. In Fig. 1c–f, the images of graphene oxide-modified TiO$_2$ does not show a clear-cut presence of the rGO flakes, however, it shows the uniform distribution of TiO$_2$ nanoparticles. The uniform distribution of TiO$_2$ nanoparticles is due to very small amount of rGO with respect to TiO$_2$ and intercalation of rGO inside the TiO$_2$ matrix. The FE-SEM investigation reveals that the crystallites are of nanometer size ranging from 36 to 56 nm.

3.2   EDXs

Figure 2 shows EDXs spectra of the prepared rGO/TiO$_2$ photocatalysts with varying concentration of rGO and GO sample. From the EDXs data, the existence of main elements such as C, O, and Ti has been observed. There is no impurity peak observed in the EDXs spectra. This confirms that the prepared samples are in pure form. The elemental composition of the GO, TiO$_2$, 5-rGO/T, 10-rGO/T, 15-rGO/T, and 20-rGO/T are depicted in Table 1.
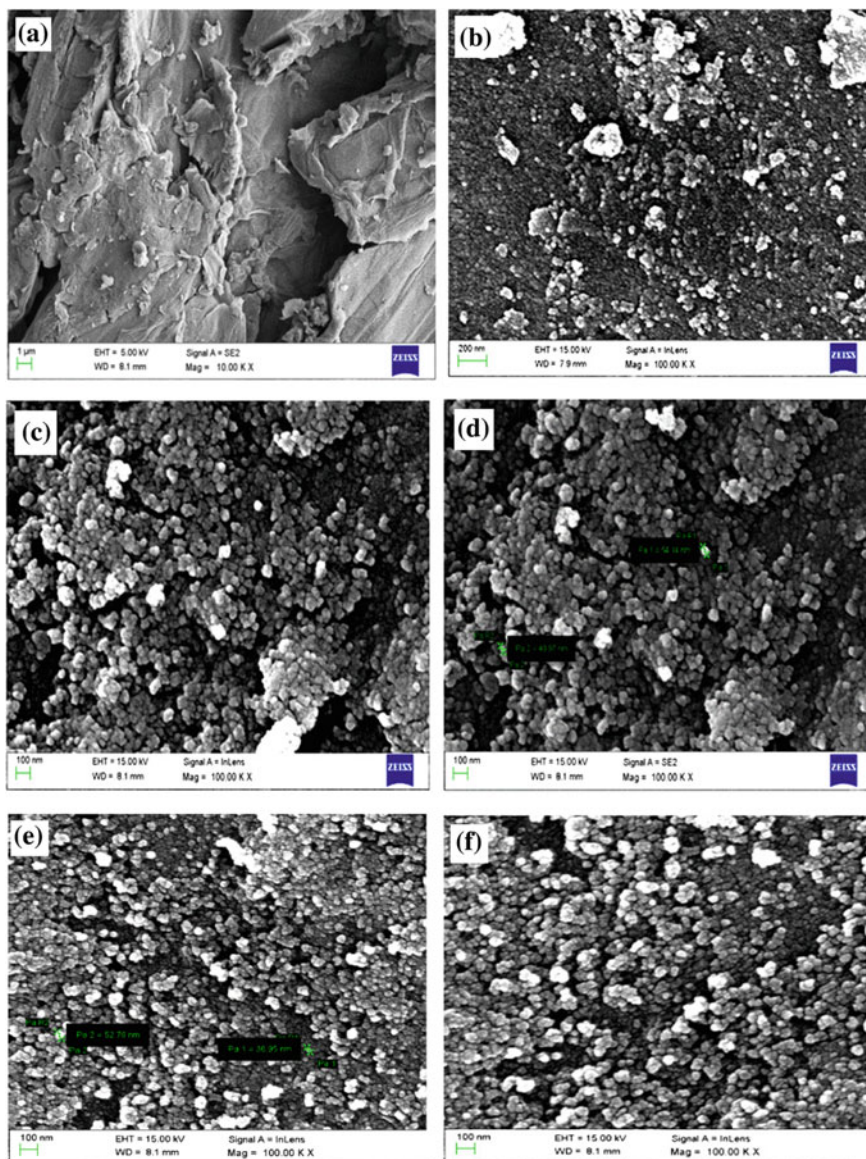
Fig. 1 FE-SEM images of different nanocomposite photocatalysts **a** GO, **b** TiO$_2$ (synthesized), **c** 5-rGO/T, **d** 10-rGO/T, **e** 15-rGO/T, **f** 20-rGO/T
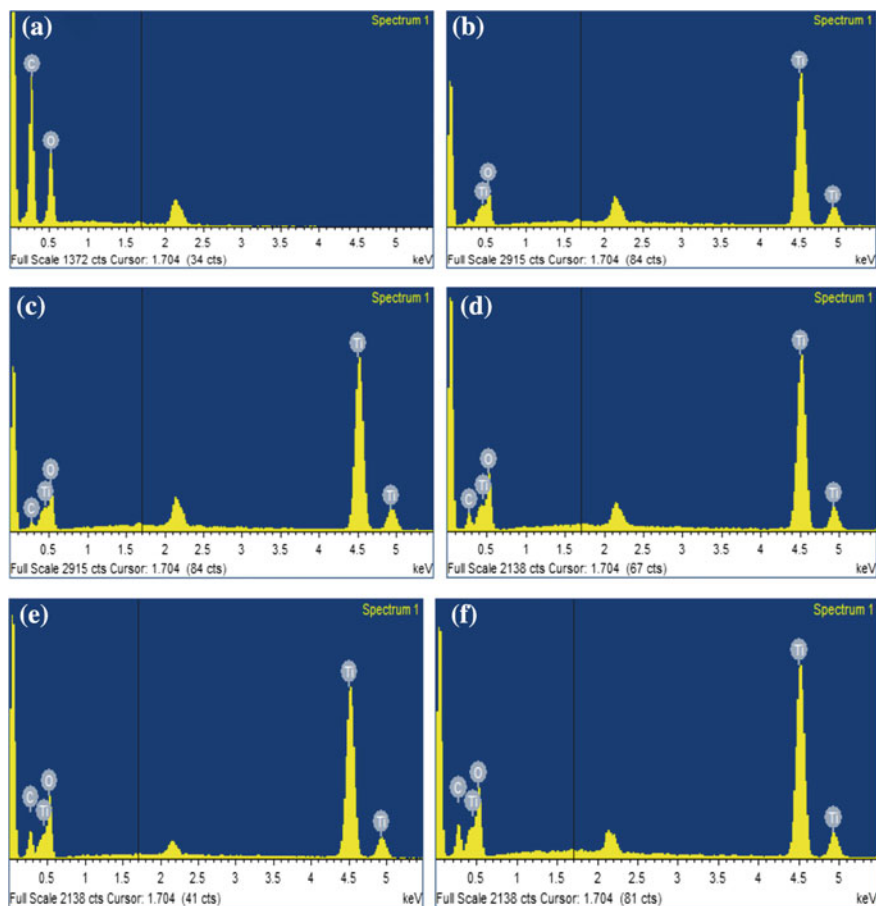
Fig. 2 EDXs elemental microanalysis of **a** GO, **b** TiO$_2$, **c** 5-rGO/T, **d** 10-rGO/T, **e** 15-rGO/T and **f** 20-rGO/T

Table 1 Surface composition from EDXs elemental microanalysis

| Sample		Element wt%			
		C	O	Ti	Total
(a)	GO	60.28	39.72	–	100
(b)	TiO$_2$	–	34.89	65.11	100
(c)	5-rGO/T	2.33	33.92	63.75	100
(d)	10-rGO/T	5.37	37.17	57.46	100
(e)	15-rGO/T	8.06	38.54	53.40	100
(f)	20-rGO/T	10.07	39.27	50.66	100

3.3 XRD Analysis

The XRD pattern of sample photocatalysts is shown in Fig. 3. The broad peaks indicate either particles of very small crystalline size, or the semi-crystalline nature. A sharp diffraction peak of GO appears at $2\theta = 11.14°$ with an interlayer spacing of 7.93 Å. The diffraction pattern of TiO_2 shows major peaks at $2\theta = 25.58, 37.20, 48.19, 54.13, 55.36, 62.89, 69.01, 70.70, 75.35$ and corresponds to the planes (101), (004), (200), (105), (211), (204), (116), (220) and (215) of anatase TiO_2, respectively (Li et al. 2014a, b). It can be observed that the intensity of the peaks attributed to rutile phase that is very small in TiO_2. The effect of rGO in TiO_2 nanocomposite found negligible and is nearly same diffraction pattern appears in all 5-rGO/T, 10-rGO/T, 15-rGO/T and 20-rGO/T photocatalysts. Since the existence of rGO in TiO_2 nanocomposite did not affect the crystalline phase of TiO_2 as shown in the XRD patterns, such interaction could be responsible for the enhanced photocatalytic performance of rGO/T.

3.4 Photocatalytic Analysis

3.4.1 Effect of Light Source

Experiments were performed under UV light source (15 W UV tube) as well as in solar light without any photocatalyst. Initially, RhB solution (10 ppm, 100 ml) was poured in a Petri dish (diameter 190 mm) and kept under illumination of UV light

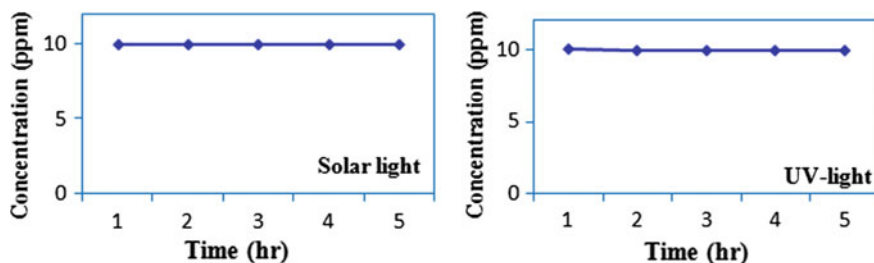**Fig. 3** XRD patterns of GO, TiO_2, 5-rGO/T, 10-rGO/T and 20-rGO/T
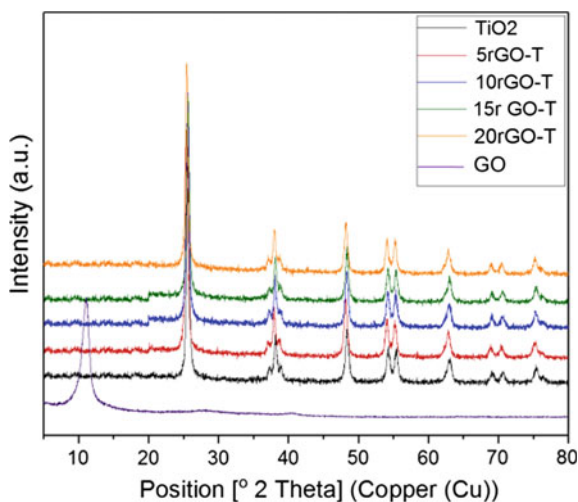
Fig. 4 Effect of light source on dye solution without any catalyst

as well as solar light. It was observed that there was no change in the concentration of RhB dye both under UV light as well as solar light (Fig. 4).

3.4.2 Catalyst Doses

The experiments were conducted to study the effect of catalyst dose for the removal of RhB dye. The best suitable dose of catalyst was determined on the basis of degradation efficiency of the unmodified TiO$_2$ photocatalyst. In these experiments, three different doses (25, 50, and 100 mg) of TiO$_2$ were taken for the same volume of dye solution (100 ml) of 10 ppm concentration. The degradation of dye was observed under both UV light as well as solar light. It can be seen from Fig. 5 that percentage degradation is high for the high value of catalyst concentration for the same time interval (3 h). The percentage degradation under UV light was obtained as 84.4%, 92.4%, and 99% for the amount of catalyst 25 mg, 50 mg, and 100 mg, respectively; whereas, the percentage degradation under solar light was 29%, 34%, and 50% for the amount of TiO$_2$ 25 mg, 50 mg, and 100 mg, respectively, which is very less. Among all three doses, 50 mg dose was selected as the best suitable dose as there is no far difference in the degradation efficiency of 50 and 100 mg dose. As we know irradiation time is also an important parameter; by seeing the above result, it can be inferred that prolonged irradiation may lead to 100% degradation of dye.

3.4.3 Effect of Type of Catalyst Under UV Light

The photocatalytic activity of all four types of photocatalysts with variable ratio of rGO to TiO$_2$ synthesized was tested to determine the optimal catalyst for RhB degradation. The catalysts 5-rGO/T, 10-rGO/T, 15-rGO/T, and 20-rGO/T with rGO content 5, 10, 15, and 20 wt%, respectively, were set under examination keeping other parameters constant. 50 mg of each sample was taken in 100 ml of the dye solution. The results are depicted in Fig. 6. The % degradation in 2.5 h for 5-rGO/T, 10-rGO/T, 15-rGO/T, and 20-rGO/T was found to be 97%, 95%, 97%, and 100%, respectively.
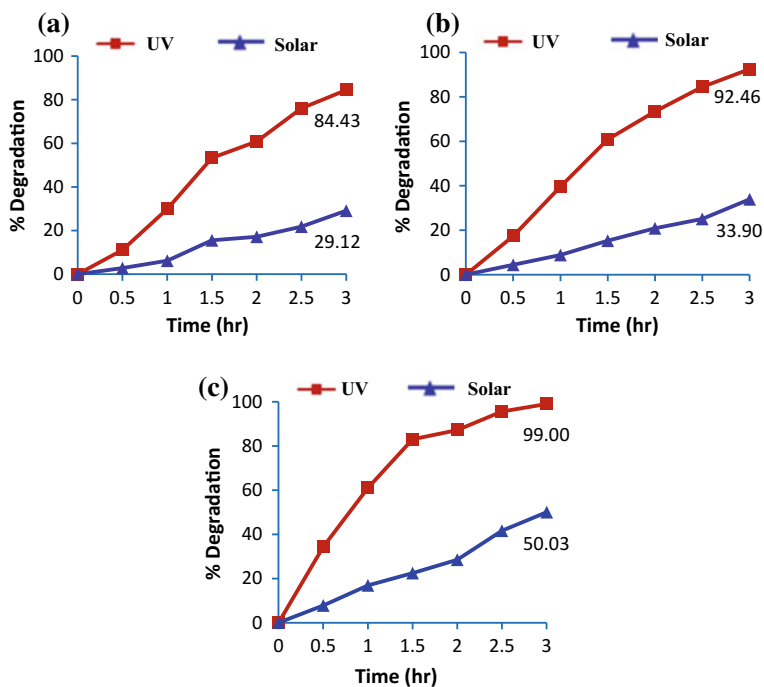
Fig. 5 Effect of catalyst dose on photocatalytic degradation of RhB (TiO$_2$ dose per 100 ml dye solution: **a** 25 mg, **b** 50 mg, **c** 100 mg)

The activity of TiO$_2$ has increased by 12–18% after modifying it with GO. The % degradation is nearly the same for 5-rGO/T and 15-rGO/T; however, there is slightly decrease in % degradation for 10-rGO/T may be due to the agglomeration of the nanocomposite. The maximum was observed for 20-rGO/T nanocomposite, which might be due to the adsorption of RhB dye as the catalyst has large surface area support. From the above results, it can be concluded that TiO$_2$ loaded with the lowest concentration of rGO (i.e., 5-rGO/T) is better among all four photocatalysts because increase in the concentration of rGO is not significantly changing the % degradation.

3.4.4 Effect of Type of Catalyst Under Solar Light

The activities of all four types of photocatalysts synthesized (5-rGO/T, 10-rGO/T, 15-rGO/T, and 20-rGO/T) were investigated under solar light keeping all the parameters the same as in under UV light. The results are shown in Fig. 7. It has been observed that the trend of degradation of RhB dye under solar light is the same as in UV light. The % degradation of RhB dye using 5-rGO/T, 10-rGO/T, 15-rGO/T and 20-rGO/T photocatalysts are 70%, 64%, 77% and 81%, respectively, whereas that of
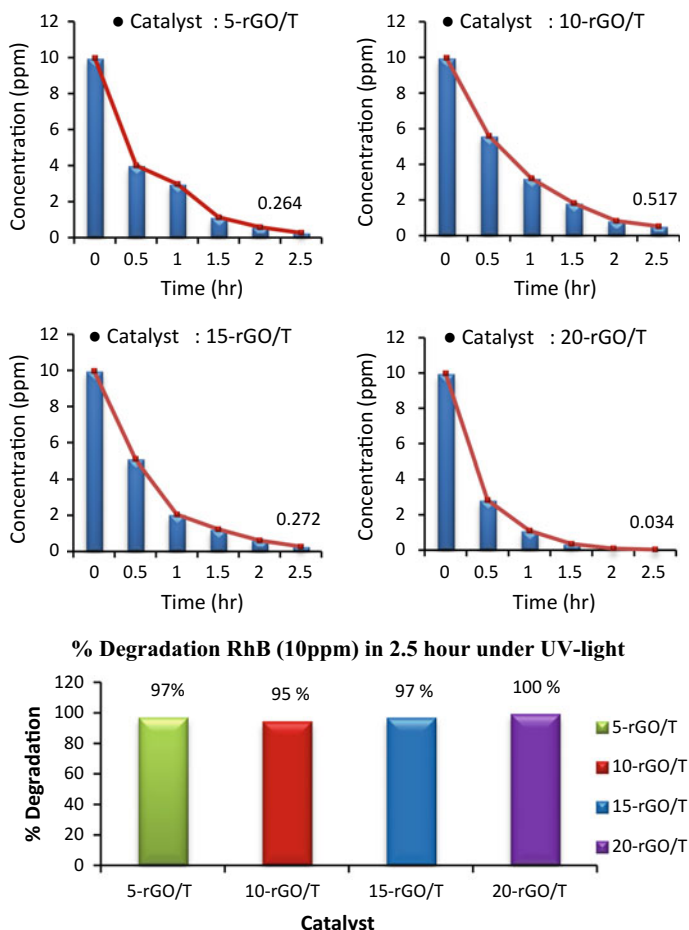
Fig. 6 Effect of type of catalyst on photocatalytic degradation of RhB (catalyst dose 50 mg/100 ml of dye solution) under UV light

bare TiO_2 is only 25%. The tremendous increase in the photocatalytic performance of rGO/TiO_2 nanocomposite can be attributed to increase in light absorption capacity and the reduction of electron-hole pair recombination in TiO_2. The characteristic feature of GO as good electron acceptor provides a flexible platform to electrons in the conduction band of TiO_2, where electrons are transferred over the surface of GO and thereby providing more time for photocatalytic reaction.
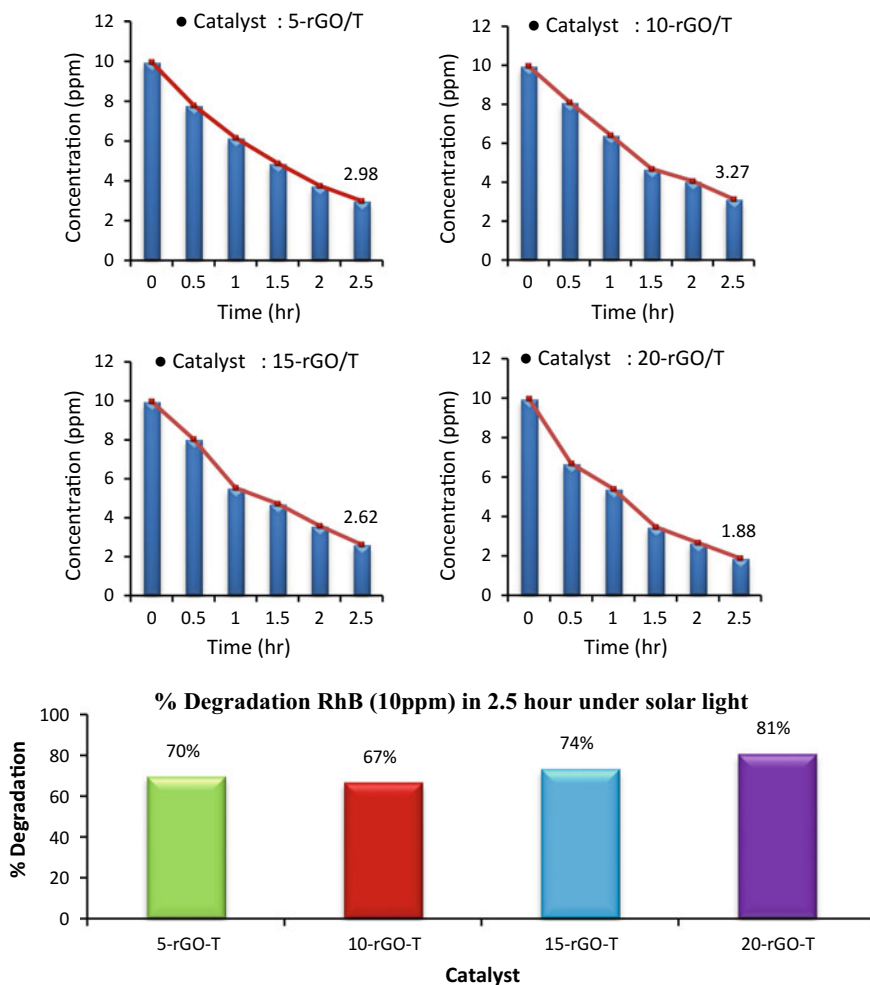
Fig. 7 Effect of type of catalyst on photocatalytic degradation of RhB (catalyst dose 50 mg/100 ml of dye solution) under solar light

3.5 Kinetic Study of Degradation of RhB Dye

The selection of a reaction system that operates in the safest and most efficient manner can be the key to the economic success or failure of a chemical process, so the kinetics study for any reaction becomes more important and necessary factor to study. The rate of reaction depends upon the number of parameters; the most important is the nature of the species involved in the reaction, concentrations of reactants and weight

Fig. 8 Kinetic degradation profile for **a** 5-rGO/T, **b** 10-rGO/T, **c** 15-rGO/T and **d** 20-rGO/T photocatalyst under UV light
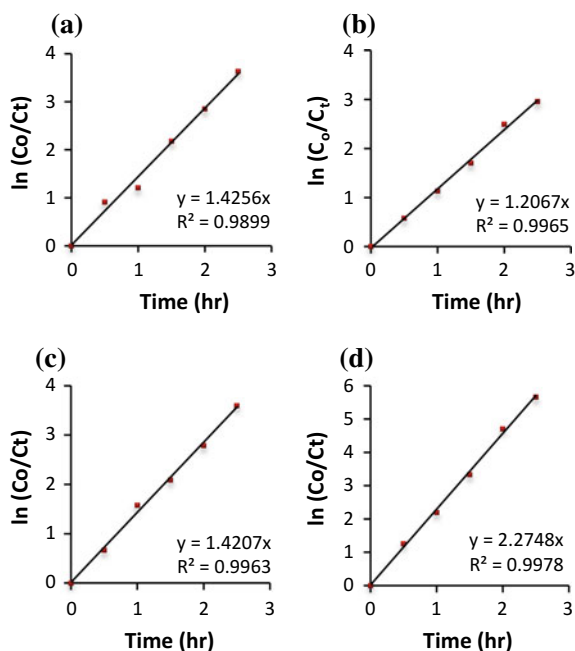
of catalyst loading in the reacting system. The plot of ln (C/C$_o$) versus time data for all the four types of photocatalysts is plotted and shown in Figs. 8a–d and 9a–d for UV light and solar light irradiation, respectively. The straight line with R^2 = 0.99 shows the best fit and indicates that the photocatalytic degradation followed the pseudo-first-order kinetics according to L-H (Langmuir-Hinshelwood) law (Li et al. 2014a, b).

Table 2 shows the pseudo-first-order reaction rate constant for all the samples in UV light and solar light. It also shows the half-life period for the degradation of RhB for all the photocatalysts and their correlation coefficient. The unmodified TiO$_2$ has the maximum half-life time (t$_{1/2}$) 0.923 h and 5.638 h under UV light and solar light respectively, which is almost 2–4 times higher than that of 5-rGO/T. After analyzing the above results, it has been found that 5-rGO/T photocatalyst showed the best fit for the pseudo-first-order reaction kinetics.

Fig. 9 Kinetic degradation profile for **a** 5-rGO/T, **b** 10-rGO/T, **c** 15-rGO/T and **d** 20-rGO/T photocatalyst under solar light
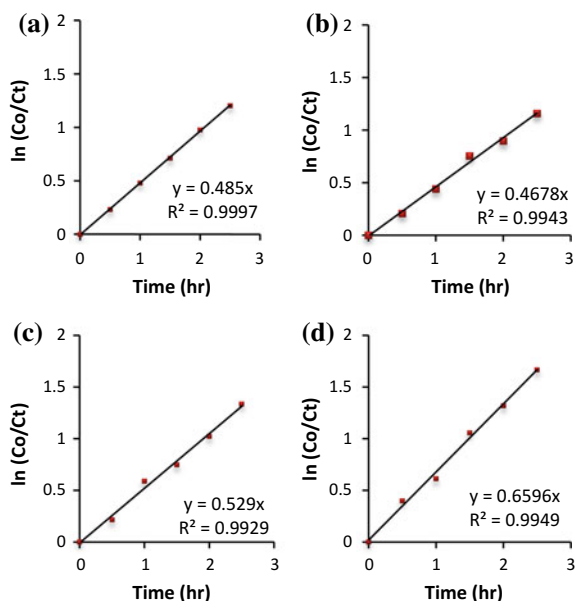

(a) graph: y = 0.485x, R² = 0.9997

(b) graph: y = 0.4678x, R² = 0.9943

(c) graph: y = 0.529x, R² = 0.9929

(d) graph: y = 0.6596x, R² = 0.9949

Table 2 Kinetic degradation coefficients for different photocatalysts

Type of sample	Under UV light			Under solar light		
	Rate const. K (h^{-1})	Half-life $t_{1/2}$ (h)	Correlation coefficient (R^2)	Rate const. K (h^{-1})	Half-life $t_{1/2}$ (h)	Correlation coefficient (R^2)
Pure TiO_2	0.751	0.923	0.988	0.123	5.638	0.9682
5-rGO/T	1.426	0.486	0.989	0.485	1.429	0.999
10-rGO/T	1.206	0.574	0.996	0.467	1.484	0.994
15-rGO/T	1.420	0.488	0.996	0.529	1.310	0.992
20-rGO/T	2.274	0.304	0.998	0.659	1.051	0.994

4 Conclusions

In this work, TiO_2 is selected as a base material for the degradation of RhB dye and was modified to enhance its photocatalytic activity. TiO_2 np was synthesized by sol–gel method. GO was prepared by the oxidation of natural graphite powder according to the modified Hummers method. The synthesis of rGO/T photocatalyst was successfully done by the photo-assisted reduction of GO using ultraviolet radiation followed by hydrothermal deposition of rGO onto the TiO_2. The synthesized photocatalysts were characterized by different physical techniques, such as X-ray diffraction, FE-SEM, and EDXs. FE-SEM analysis reflected the morphology of GO as layered structure and that of TiO_2 and rGO/T as spherical structure. The XRD

spectra confirmed crystalline nature of TiO_2 and rGO/T, with anatase being the main crystalline phase. The introduction of GO over the TiO_2 np reflected no change in the crystalline phase of GO modified TiO_2 nanocomposites. The results of photocatalytic degradation of RhB dye showed an improvement in the degradation efficiency of rGO/T photocatalysts by almost two–three times that of pure TiO_2. From the experimental data, it has been concluded that 5-rGO/T having 5% GO content is best among all the photocatalysts synthesized. The rate of photodegradation of RhB was successfully fitted by Langmuir–Hinshelwood kinetic model. RhB dye followed the pseudo-first-order reaction kinetics for photodegradation. This study explored the feasibility of using sunlight as the main light source for photocatalytic degradation of organic dye.

References

Abdel-Messih M, Ahmed M, El-Sayed A (2013) Photocatalytic decolorization of Rhodamine B dye using novel mesoporous SnO_2–TiO_2 nano mixed oxides prepared by sol–gel method. J Photochem Photobiol A 260:1–8. https://doi.org/10.1016/j.jphotochem.2013.03.011

Carneiro J, Samantilleke A, Parpot P et al (2016) Visible light induced enhanced photocatalytic degradation of industrial effluents (Rhodamine B) in aqueous media using TiO_2 nanoparticles. J Nanomater 2016:1–13. https://doi.org/10.1155/2016/4396175

Chang W, Shen Y, Xie A, Tong W (2009) Preparation of Al_2O_3-supported nano-Cu_2O catalysts for the oxidative treatment of industrial wastewater. Russ J Phys Chem A 83:2308–2312. https://doi.org/10.1134/s0036024409130214

Chen X, Mao S (2007) Titanium dioxide nanomaterials: synthesis, properties, modifications, and applications. ChemInform. https://doi.org/10.1002/chin.200741216

Dubey P, Tripathi P, Tiwari R et al (2014) Synthesis of reduced graphene oxide–TiO_2 nanoparticle composite systems and its application in hydrogen production. Int J Hydrogen Energy 39:16282–16292. https://doi.org/10.1016/j.ijhydene.2014.03.104

Fang W, Xing M, Zhang J (2017) Modifications on reduced titanium dioxide photocatalysts: a review. J Photochem Photobiol C 32:21–39. https://doi.org/10.1016/j.jphotochemrev.2017.05.003

Friedmann D, Mendive C, Bahnemann D (2010) TiO2 for water treatment: parameters affecting the kinetics and mechanisms of photocatalysis. Appl Catal B 99:398–406. https://doi.org/10.1016/j.apcatb.2010.05.014

Gnanasekaran L, Hemamalini R, Ravichandran K (2015) Synthesis and characterization of TiO_2 quantum dots for photocatalytic application. J Saudi Chem Soc 19:589–594. https://doi.org/10.1016/j.jscs.2015.05.002

Hamandi M, Berhault G, Guillard C, Kochkar H (2017) Reduced graphene oxide/TiO_2 nanotube composites for formic acid photodegradation. Appl Catal B 209:203–213. https://doi.org/10.1016/j.apcatb.2017.02.062

Krejčíková S, Matějová L, Kočí K et al (2012) Preparation and characterization of Ag-doped crystalline titania for photocatalysis applications. Appl Catal B 111–112:119–125. https://doi.org/10.1016/j.apcatb.2011.09.024

Kumar K, Kumar G, Reddy K (2015) Rapid microwave synthesis of reduced graphene oxide-supported TiO_2 nanostructures as high performance photocatalyst. Mater Today Proc 2:3736–3742. https://doi.org/10.1016/j.matpr.2015.07.204

Li D, Zheng H, Wang Q et al (2014a) A novel double-cylindrical-shell photoreactor immobilized with monolayer TiO_2-coated silica gel beads for photocatalytic degradation of Rhodamine B and

Methyl Orange in aqueous solution. Sep Purif Technol 123:130–138. https://doi.org/10.1016/j.seppur.2013.12.029

Li Y, Yan J, Su Q et al (2014b) Preparation of Graphene–TiO$_2$ nanotubes/nanofibers composites as an enhanced visible light photocatalyst using a hybrid synthetic strategy. Mater Sci Semicond Process 27:695–701. https://doi.org/10.1016/j.mssp.2014.08.001

Lin W, Liao C, Chang T et al (2015) Humidity sensing properties of novel graphene/TiO$_2$ composites by sol–gel process. Sens Actuators B Chem 209:555–561. https://doi.org/10.1016/j.snb.2014.12.013

Lorestani F, Shahnavaz Z, Mn P et al (2015) One-step hydrothermal green synthesis of silver nanoparticle-carbon nanotube reduced-graphene oxide composite and its application as hydrogen peroxide sensor. Sens Actuators B Chem 208:389–398. https://doi.org/10.1016/j.snb.2014.11.074

Lv X, Zhang G, Fu W (2012) Highly efficient hydrogen evolution using TiO$_2$/graphene composite photocatalysts. Procedia Eng 27:570–576. https://doi.org/10.1016/j.proeng.2011.12.489

Nakata K, Fujishima A (2012) TiO$_2$ photocatalysis: design and applications. J Photochem Photobiol C 13:169–189. https://doi.org/10.1016/j.jphotochemrev.2012.06.001

Oseghe E, Ndungu P, Jonnalagadda S (2014) Synthesis of mesoporous Mn/TiO$_2$ nanocomposites and investigating the photocatalytic properties in aqueous systems. Environ Sci Pollut Res 22:211–222. https://doi.org/10.1007/s11356-014-3356-z

Rani S, Aggarwal M, Kumar M et al (2016) Removal of methylene blue and rhodamine B from water by zirconium oxide/graphene. Water Sci 30:51–60. https://doi.org/10.1016/j.wsj.2016.04.001

Shao X, Lu W, Zhang R, Pan F (2013) Enhanced photocatalytic activity of TiO$_2$-C hybrid aerogels for methylene blue degradation. Scientific Reports. https://doi.org/10.1038/srep03018

Shen K, Gondal M (2017) Removal of hazardous Rhodamine dye from water by adsorption onto exhausted coffee ground. J Saudi Chem Soc 21:S120–S127. https://doi.org/10.1016/j.jscs.2013.11.005

Štengl V, Bakardjieva S, Grygar T et al (2013) TiO$_2$-graphene oxide nanocomposite as advanced photocatalytic materials. Chem Cent J 7:41. https://doi.org/10.1186/1752-153x-7-41

Thiruvenkatachari R, Vigneswaran S, Moon I (2008) A review on UV/TiO$_2$ photocatalytic oxidation process (Journal Review). Korean J Chem Eng 25:64–72. https://doi.org/10.1007/s11814-008-0011-8

Yadav M, Yadav A, Fernandes R et al (2017) Tungsten-doped TiO$_2$/reduced Graphene Oxide nanocomposite photocatalyst for degradation of phenol: a system to reduce surface and bulk electron-hole recombination. J Environ Manag 203:364–374. https://doi.org/10.1016/j.jenvman.2017.08.010

Yu D, Cai R, Liu Z (2004) Studies on the photodegradation of Rhodamine dyes on nanometer-sized zinc oxide. Spectrochim Acta Part A Mol Biomol Spectrosc 60:1617–1624. https://doi.org/10.1016/j.saa.2003.09.00